

Materials science communication

Surface potential analysis on initial galvanic corrosion of Ti/Mg-Al dissimilar material



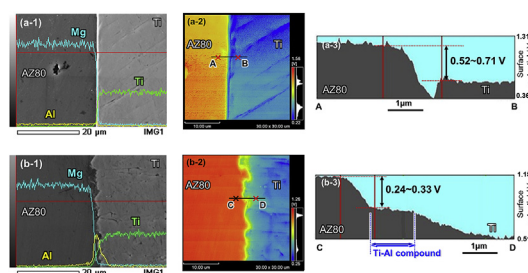
Junko Umeda, Nozomi Nakanishi, Katsuyoshi Kondoh*, Hisashi Imai

Joining and Welding Research Institute, Osaka University, 11-1 Mihogaoka, Ibaragi, Osaka 567-0047, Japan

HIGHLIGHTS

- Pure Ti/AZ80 Mg alloy dissimilar material was prepared by spark plasma sintering.
- Additional heat treatment caused a formation of Ti-Al interlayer.
- Significant decrease of potential difference of 0.24–0.33 V was found at interface.
- Heat treated dissimilar material showed very few Mg(OH)₂ debris after salt water immersion test.

GRAPHICAL ABSTRACT



ARTICLE INFO

Article history:

Received 21 December 2015

Received in revised form

6 May 2016

Accepted 11 May 2016

Available online 24 May 2016

Keywords:

Intermetallic compounds

Interfaces

Corrosion test

Diffusion

ABSTRACT

A surface potential analysis was carried out to establish a new materials design of pure Ti/Mg-Al alloy dissimilar materials with an excellent galvanic corrosion resistance. The formation of Ti-Al intermetallic interlayer and Al diffusion layer at interface effectively reduced the surface potential difference at the interface. As a result, a formation of local cells, causing a galvanic corrosion phenomenon of Ti/Mg alloy dissimilar material, was prevented because the potential difference of Mg alloy with Ti-Al interlayer completely decreased. A salt water immersion test obviously indicated no Mg(OH)₂ corrosion product on Mg alloy surface due to Ti-Al interlayer formation, and the initial galvanic corrosion phenomenon was effectively obstructed.

© 2016 Elsevier B.V. All rights reserved.

1. Introduction

A multi-materials design is widely applied to automotive and aerospace components to realize both significant weight reduction and strength improvement at the same time. The dissimilar material by joining the different materials plays an important role to obtain many advantages such as downsizing, cost reduction, and high-performance of the components. Al/steel [1], Mg/steel [2], and Ti/steel [3] dissimilar jointed materials are representative

combinations in the industrial application. A dissimilar material consisting of Ti and Mg alloys has a large potential for weight reduction because both metals show high specific strength and specific Young's modulus compared to the other industrial metals. This also has a possibility to be employed as lightweight reinforcements of aircrafts. With regard to the bonding ability of Ti to Mg, the previous study shows a good wettability of pure Ti by molten pure Mg because of Ti plate surface modification after TiO₂ layer chemically reduced by contact with molten Mg [4]. A fibre laser welding process was one of the suitable joining techniques to prepare this unique dissimilar material [5]. In this combination, however, there are two important problems in joining; a small solid

* Corresponding author.

E-mail address: kondoh@jwri.osaka-u.ac.jp (K. Kondoh).

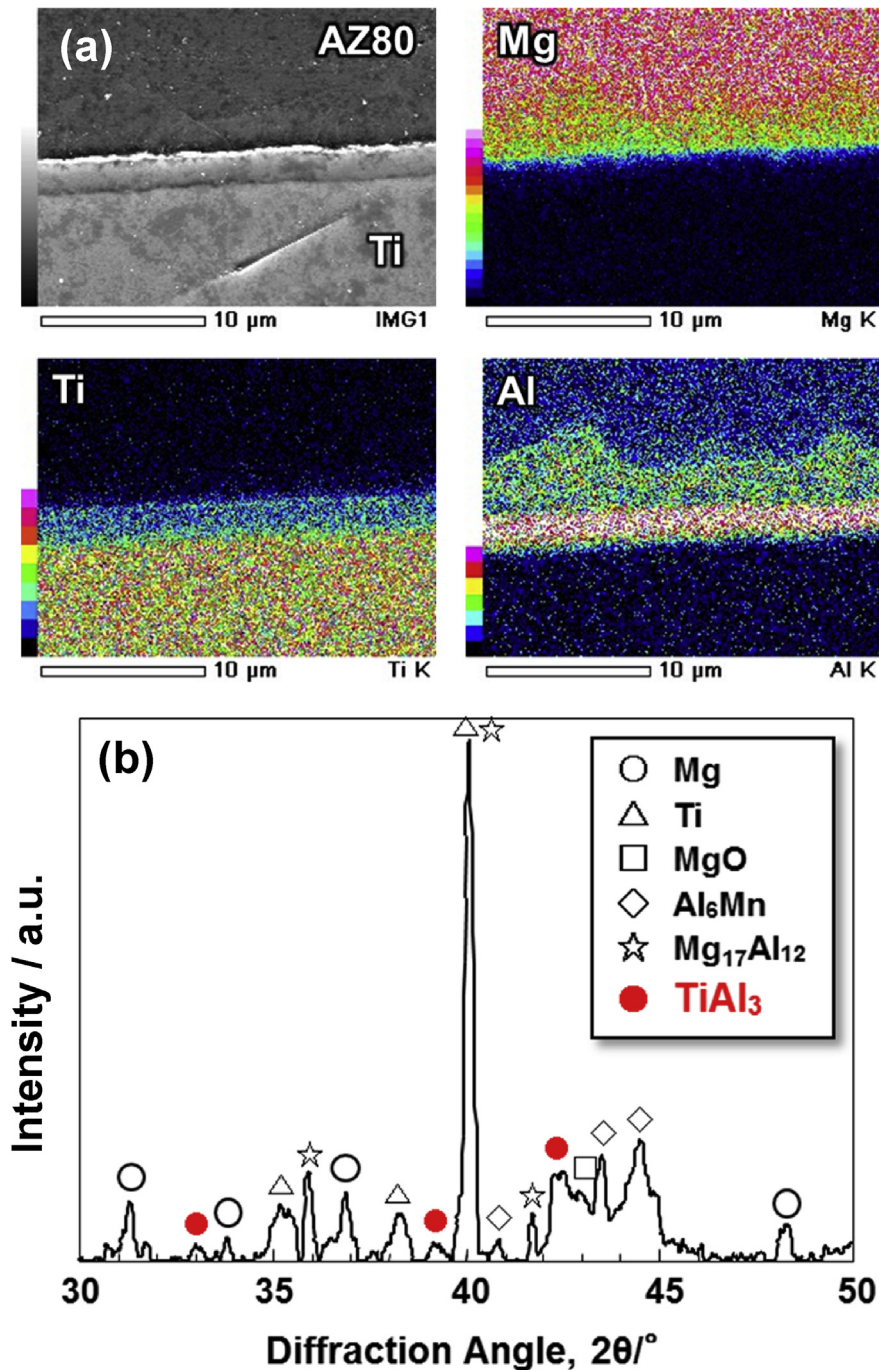


Fig. 1. SEM-EDS analysis results (a) and XRD profile (b) near interface of pure Ti/AZ80 dissimilar material after heat treatment at 1073 K for 1.8 ks in vacuum (-6 Pa). TiAl_3 intermetallic compound inter layer and Al concentrated area are formed via reaction between Ti and Al elements from molten AZ80 alloy.

solubility of Ti in Mg and that of Mg in Ti, and a large melting point difference between pure Mg and pure Ti (1019 K) [6]. In addition, the Al content contained as a strengthening alloying element in Ti and Mg alloys has a significant effect on the interfacial properties of the dissimilar material. For example, microstructures and mechanical strength depend on the formation of Mg-Al eutectic phases [7] and Ti-Al intermetallic compounds [8] near the interface of the Ti/Mg dissimilar material. From a viewpoint of galvanic corrosion originated in the local cells at interfaces of the dissimilar material, a large difference of the standard electrode potential between Ti (-1.63 V) and Mg (-2.35 V) possibly causes a galvanic

corrosion phenomenon [9]. The galvanic corrosion is also influenced by the Al concentration near the interface because of Mg-Al phase formation and Al solid-solution into α -Mg matrix [10].

In this study, the initial galvanic corrosion behavior at the interface of pure Ti/AZ80 (Mg-Al) alloy dissimilar material prepared by spark plasma sintering (SPS) in solid-state and the following heat treatment was investigated by surface potential difference measurement using scanning Kelvin probe force microscopy (SKPFM) system [11–13]. The previous study showed that SKPFM measurement results were useful to estimate the corrosion potentials of materials because a linear relationship between the work functions

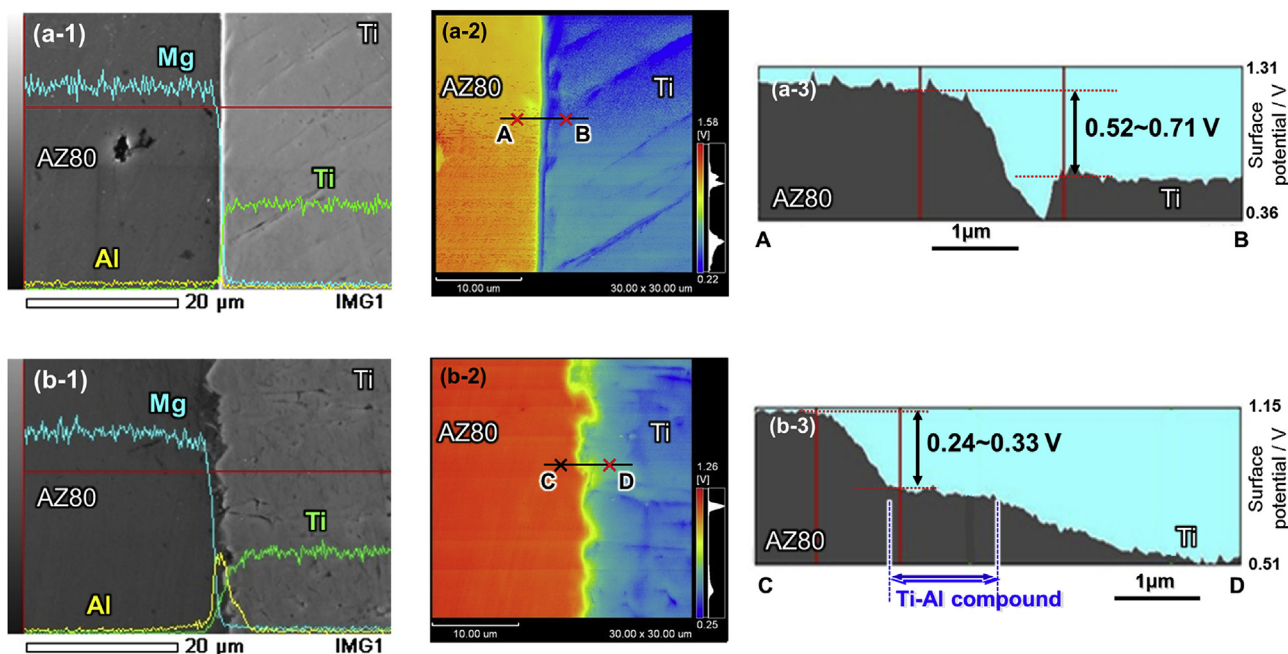


Fig. 2. Mg, Ti and Al element distribution measured by EDS line-analysis and surface potential distribution mapping analyzed by SKPFM of Sample I (a) and Sample II (b). Sample I shows never Al diffused and concentrated area at Ti/AZ80 interface, and a large potential difference of 0.52–0.71 V at the interface. Sample II obviously reveals Al diffusion from AZ80 into pure Ti, and a stepwise change in surface potential at the interface. In particular, AZ80 alloy shows a small potential drop of 0.24–0.33 V due to TiAl₃ compound interlayer formation.

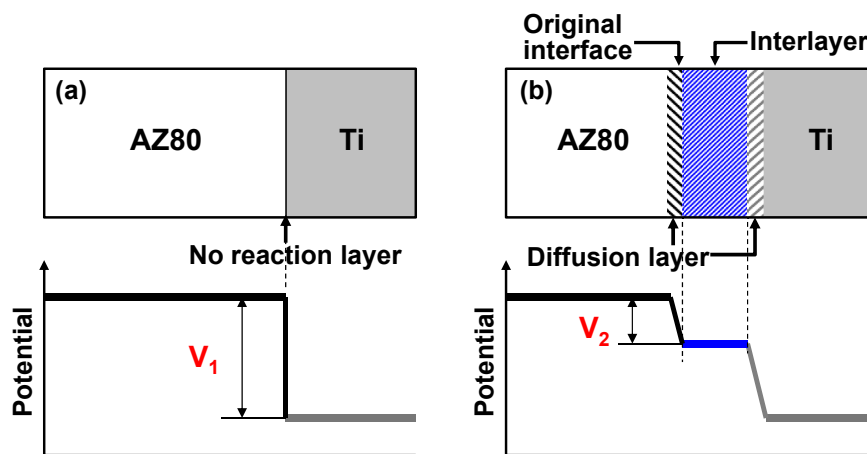


Fig. 3. Schematic illustration of surface potential changes near Ti/AZ80 interface without reaction layer, Sample I (a) and with interlayer and diffusion area, Sample II (b) of pure Ti/AZ80 dissimilar material. A large surface potential difference (V₁) in Sample I is certainly reduced due to formation of interlayer and diffusion layer by Al elements originated from AZ80 alloy, and results in a small potential drop (V₂) in Sample II.

by SKPFM and corrosion potentials of pure metals and intermetallic compounds was clearly found [14]. In addition, the potential difference measured by SKPFM was applied to evaluate the local corrosion phenomenon of cold-rolled stainless steels [15]. The effect of Al elements originated from AZ80 alloy on the interlayer formation and surface potential distribution at the interface, which affected galvanic corrosion phenomena, was discussed. In addition, the morphology observation on the dissimilar specimen surface after salt water immersion test was also carried out in this study.

2. Experimental procedure

Disk-shaped specimens of Mg-7.8Al-0.68Zn-0.18Mn (AZ80) alloy (in mass%) after homogenization at 688 K for 24 h and pure Ti (purity; 99.5%) were put in a carbon die (inner diameter of 41 mm)

installed in the SPS equipment. 40 MPa pressure was applied to bond them at 673 K for 2 h in vacuum (~6 Pa). As-joined Ti/AZ80 dissimilar material (Sample I) was served to the following heat treatment at 1073 K for 0.5 h in argon gas atmosphere to synthesize Ti-Al intermetallic layers at the bonding interface. This is because the heating temperature is much higher than the melting point of AZ80 alloy and effective enough to their compounds formation by the active liquid state diffusion of Al elements originated in AZ80 alloy [8]. Scanning electron microscope (SEM) with energy-dispersive X-ray spectroscopy (EDS) analysis was carried out to investigate the interfacial microstructures of the dissimilar material, in particular, the formation of Ti-Al interlayer and Al diffusion layer in pure Ti. Scanning Kelvin probe force microscope (SKPFM) analysis was conducted to directly measure the surface potential drop at the interface causing the initial galvanic corrosion. In

addition, a salt water immersion test was performed to analyze a formation of surface corrosion products of AZ80 alloy by using 5 wt % NaCl solution, where the solution temperature was 303 K and soaking time was 3 h. SEM-EDS analysis was conducted to examine the surface changes and corrosion damages near the joined interface after the above corrosion immersion test.

3. Results and discussion

Fig. 1 (a) reveals an interlayer formation with about 2 μm thickness at the interface between AZ80 and pure Ti of the dissimilar material after the above heat treatment (Sample II) by scanning electron microscopy (SEM). Al elements concentrated at the layer are also detected by energy-dispersive X-ray spectroscopy (EDS) analysis. In addition, the diffused Al elements area close to the interface, but no Ti diffusion into AZ80 side is found after heat treatment. X-ray diffraction (XRD) analysis in (b) obviously shows some diffraction peaks of not only Ti, Mg, MgO, $\text{Mg}_{17}\text{Al}_{12}$ (eutectic), Al_6Mn originated from the raw materials, but also in-situ formed TiAl_3 compounds during heat treatment, which are most thermally stable at 1073 K in Ti–Al phases [16], near the interface.

Fig. 2 indicates SEM-EDS and SKPFM analysis on Samples I and II. In Sample I, neither Al diffusion nor interlayer formation at the bonding interface is observed in SEM photo with EDS-line analysis result (a-1). This is because SPS temperature of 673 K, which is lower than that in the homogenization treatment (688 K), is not effective to Al diffusion of AZ80 alloy. In addition, the bonding interface is very flat and smooth compared to Sample II due to no metallurgical reaction between these metals in Sample I. SKPFM

was conducted at the same area in (a-1) to measure the surface potential distribution near the bonding interface. As shown in (a-2) and (a-3), the potential at AZ80 specimen is much higher than that of pure Ti, and drastically decreases at the interface, where the potential drop is 0.52–0.71 V (average at 4 measurement; 0.62 V). On the other hand, as shown in Fig. 2 (b-1) of Sample II, it evidently reveals not only the concentrated Al elements at the interface but also the uneven interface after heat treatment because of the metallurgical bonding after the chemical reduction of TiO_2 surface film of pure Ti specimen by liquid Mg elements [4]. Regarding the surface potential distribution mapping, a stepwise change in the potential near the interface was detected in (b-3). It means the gradual slopes from AZ80 to the interface and from the interface to pure Ti specimen were clearly observed. The formation of TiAl_3 reaction layer, having a constant potential of 0.79–0.84 V, interrupts the direct bonding of AZ80 alloy to pure Ti, and results in a small potential drop (0.24–0.33 V) of AZ80 specimen near the interface. Fig. 3 schematically illustrates the potential changes near the interface of pure Ti/AZ80 dissimilar materials with no reaction layer, Sample I (a) and with Ti–Al interlayer and Al diffusion layer, Sample II (b). It is concluded that the interlayer formation between AZ80 and pure Ti by heat treatment in Sample II effectively decreases a surface potential difference at the interface, which causes local cells to accelerate the galvanic corrosion phenomenon.

Fig. 4 presents the surface morphology changes of each Ti/AZ80 dissimilar material after the salt water immersion corrosion test observed by SEM-EDS analysis. In general, Mg easily resolves into an aqueous solution, and magnesium hydroxide ($\text{Mg}(\text{OH})_2$) films are formed as corrosion products on Mg specimen surface via

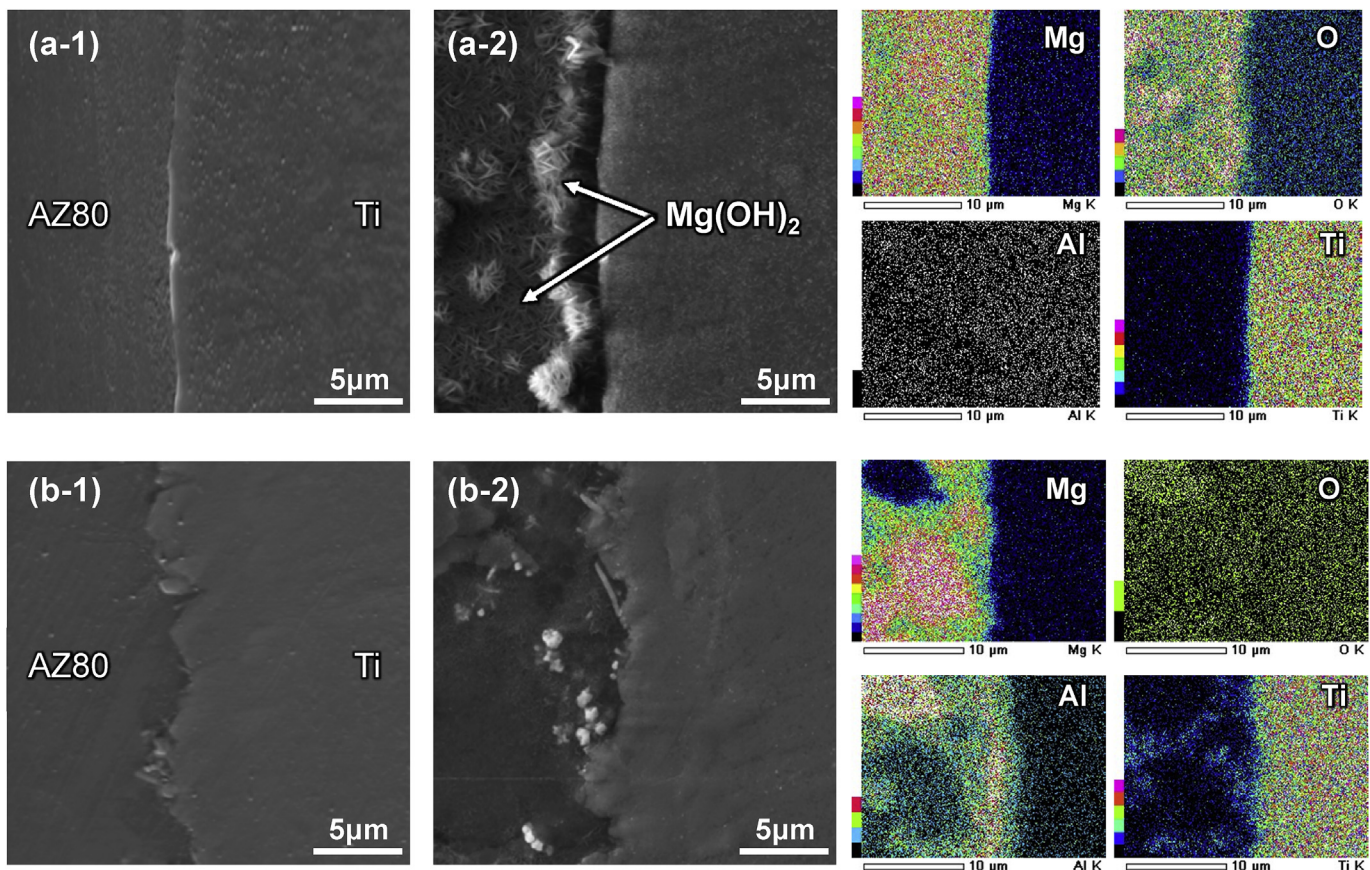


Fig. 4. Surface morphology changes near pure Ti/AZ80 interface of Sample I (a) and Sample II (b) by salt water immersion test, and SEM-EDS analysis results of each specimen. $\text{Mg}(\text{OH})_2$ corrosion products and oxygen elements concentration are obviously observed on AZ80 alloy surface of Sample I. In Sample II, very few corrosion products are detected near the interface after immersion corrosion test.

general whole surface corrosion phenomena [17]. Additionally, when a large potential difference at the interface between intermetallic compounds and α -Mg matrix occurs, it also causes a galvanic corrosion phenomenon with $\text{Mg}(\text{OH})_2$ formation [18–20]. Fig. 4 (a-1) and (b-1) indicate no $\text{Mg}(\text{OH})_2$ formation on AZ80 alloy in both samples before the corrosion test. As shown in (a-2), however, $\text{Mg}(\text{OH})_2$ corrosion products are obviously detected on AZ80 surface near the interface of Sample I after corrosion test. EDS analysis result also reveals the concentrated oxygen elements originated from $\text{Mg}(\text{OH})_2$ at AZ80 surface. The potential difference of 0.52–0.71 V at the interface shown in Fig. 2 (a-3) is almost the same as that in a combination of Mg with pure Cu (0.33–0.68 V) and pure Fe (0.80–0.87 V) measured by SKPFM. It is well known a small addition of Cu and Fe elements as impurities in Mg materials causes a severe galvanic local corrosion [21]. Then, it is concluded that such a large potential difference in Sample I is enough for an acceleration of the galvanic phenomenon and results in formation of many corrosion products on AZ80 surface near the interface shown in Fig. 4 (a-2). On the other hand, (b-2) indicates very few corrosion products in AZ80 alloy near the interface of Sample II after corrosion test, and no concentration of oxygen is detected at the interface. In the previous studies on the surface potential difference measurement between intermetallic compounds and Mg matrix by using SKPFM system, the average of Mg with $\text{Mg}_{17}\text{Al}_{12}$ and Al_8Mn_5 , which are commonly contained in the commercial Mg alloys, are 0.15 V and 0.26 V, respectively [22,23]. It is also well opened that these compounds have no effect on the galvanic acceleration of the conventional Mg alloys. It means the potential difference in the above range hardly causes a galvanic corrosion of Mg alloys. A small potential drop (0.24–0.33 V) at the interface by both TiAl_3 interlayer formation and Al concentration in Sample II shown in Fig. 2 (b-3) is not effective in inducing the galvanic corrosion, and results in very few $\text{Mg}(\text{OH})_2$ corrosion products formation as shown in Fig. 4 (b-2).

4. Conclusions

The pure Ti/AZ80 bonded dissimilar material prepared by SPS in solid-state had no formation of Ti-Al intermetallic compound layer

at the interface. The additional heat treatment at 1073 K to the dissimilar material affected the interlayer formation and Al diffusion near the bonding interface. In the former material, a large potential drop of 0.52–0.71 V at the interface was measured by SKPFM, and caused many corrosion products of $\text{Mg}(\text{OH})_2$ debris by galvanic local corrosion phenomenon. The latter with the interlayers showed a significant decrease of the potential difference with 0.24–0.33 V at the interface, and resulted in preventing the galvanic corrosion of AZ80 specimen.

References

- [1] C. Rest, P.J. Jacques, A. Simar, *Scr. Mater.* 77 (2014) 25–28.
- [2] Y.C. Chen, K. Nakata, *Mater. Des.* 30 (2009) 3913–3919.
- [3] M. Kutsuna, R. Ichioka, *Weld. World* 51 (2007) 5–8.
- [4] K. Kondoh, M. Kawakami, H. Imai, J. Umeda, H. Fujii, *Acta Mater.* 58 (2010) 606–614.
- [5] M. Gao, Z.M. Wang, J. Yan, X.Y. Zen, *Sci. Tech. Weld. Join.* 16 (2011) 488–496.
- [6] J.L. Murray, *Phase Diagrams of Binary Titanium Alloys*, ASM International, Materials Park, OH, 1998.
- [7] J.L. Murray, *Bull. Alloy Phase Diagrams* 3 (1982) 60–74.
- [8] J.H. Westbrook, R.L. Fleischer, *Intermetallic Compounds*, John Wiley & Sons, NY, 2000.
- [9] P.W. Atkins, *Physical Chemistry*, sixth ed., Oxford University Press, Oxford, 1998, pp. 934–936.
- [10] L.Y. Mei, G.L. Dunlop, H. Westengen, *J. Mater. Sci.* 31 (1996) 387–397.
- [11] M. Nonnenmacher, M.P. Boyle, H.K. Wickramasinghe, *Kelvin probe force microscopy*, *Appl. Phys. Lett.* 58 (1991) 2921–2923.
- [12] P. Schmutz, G.S. Frankel, *J. Electrochem. Soc.* 145 (1998) 2285–2295.
- [13] H. Fukuda, J.A. Szpunar, K. Kondoh, R. Chromik, *Corros. Sci.* 52 (2010) 3917–3923.
- [14] R. Takei, H. Imai, J. Umeda, K. Kondoh, *Trans. JWRI* 39 (2010) 75–80.
- [15] C. Örnek, D.L. Engelberg, *Corros. Sci.* 99 (2015) 164–171.
- [16] J. Speight, J.G. Speight, N.A. Lange, J.A. Dean, *Lange's Handbook of Chemistry*, McGraw-Hill Scientific, NY, 1999.
- [17] J. Van Muylder, M. Pourbaix, *Magnesium*, Pergamon Press, Oxford, 1966.
- [18] J.X. Jia, A. Atrens, G. Song, T.H. Muster, *Mater. Corros. Werkst. Korros.* 56 (2005) 468–474.
- [19] M. Jonsson, D. Thierry, N. LeBozec, *Corros. Sci.* 48 (2006) 1193–1208.
- [20] R. Takei, H. Imai, J. Umeda, K. Kondoh, *Trans. JWRI* 39 (2010) 75–80.
- [21] G.L. Maker, J. Kruger, *Inter. Mater. Rev.* 38 (1993) 138–153.
- [22] F. Andreatta, I. Apachitei, A.A. Kodentsov, J. Dzwonczyk, J. Duszczak, *Electrochim. Acta* 51 (2006) 3551–3557.
- [23] D.B. Blucher, J.E. Svensson, L.G. Johansson, M. Rohwerder, M. Stratmann, *J. Electrochem. Soc.* 151 (2004) B621–B626.